BIOCHEMISTRY
including biophysical chemistry & molecular biology
Article

Biochemistry **2009,** *48,* 12265–12271 12265
DOI: 10.1021/bi901514h

Application of the Second Rule of Transient-State Kinetic Isotope Effects to an Enzymatic Mechanism†

Harvey F. Fisher,* Steven J. Maniscalco, Jon Tally, and Kayann Tabanor

The Department of Biochemistry, University of Kansas Medical Center, 3901 Rainbow Boulevard, Kansas City, Kansas 66160

Received August 28, 2009; Revised Manuscript Received November 19, 2009

ABSTRACT: The transient-state kinetic approach reveals the formation and subsequent interconversions of intermediates in real time. Its potential for the mechanistic resolution of enzymatic and other complex chemical mechanisms has been severely limited however by the lack of a rigorous and applicable theoretical basis in contrast to that of the less direct but soundly based algebraic algorithms of the steady-state approach. Having recently established three rigorously derived fundamental "rules" of transient-state kinetics applicable to realistic multiple step reactions, we present here the successful application of the very counterintuitive "second rule" to the resolution of the mechanism of the L-phenylalanine dehydrogenase catalyzed reaction.

The steady-state kinetic approach has provided the overwhelming portion of what we now know about the mechanisms of enzymatic catalysis. While any such experiment provides only a single pair of parameters (V and V/K_m), their interpretation rests on a large body of rigorously derived algebraic formulations. Variation of pH, reactant and product concentrations, and kinetic isotope effects (KIEs)[1] combined with X-ray crystallographic structures has produced many detailed mechanisms interpretable in terms of physical−organic chemical theory (*1*). Yet, we are still a very long way from a thorough understanding of the phenomenon of enzymatic catalysis.

In contrast to the steady-state approach, transient-state kinetic experiments typically provide a wide variety of optical phenomena tracking the formation and interconversions of enzyme-bound intermediates in real time. The effectiveness of the transient (pre-steady-state) approach, however, has been severely limited by the lack of a coherent body of rigorous analytical theorems applicable to the results of transient-state (stopped-flow) experimental data (*2*). The necessity of interpreting our experimental results has led us to develop such a theory.

Kinetic isotope effects (KIEs) are an important tool for the steady-state kineticist (*3*). By definition, a steady-state KIE is defined as a single value at zero time. In contrast, transient-state KIEs (tKIEs) are strongly time dependent and may be presumed to contain significantly more extensive mechanistic information. To our knowledge, no analytic theory applicable to realistic enzyme mechanisms for tKIEs existed prior to this report. Experimental and theoretical developments described here have now provided a solid basis for the development of such a body of theory.

On the basis of the results of transient-state kinetic experiments involving a single-step deuterium substitution on an amino acid α-carbon atom, followed by extensive simulation by numerical integration and subsequent rigorous mathematical proof, we have recently announced the three fundamental "rules" of transient-state kinetic isotope effects (*4*). Recognizing from experimental data that even in such single-step substituted cases isotope effects occur on each and every succeeding step of the reaction and that all such effects are time dependent, we define a transient-state kinetic isotope effect for any given reaction component, X, as $tKIE_{x,t} = \frac{d[X_H]/dt}{d[X_D]/dt}$ where H and D refer to the unsubstituted and the isotope-substituted reactions, respectively. [This definition is analogous to the time-independent form of its steady-state counterpart, $KIE = (d[P_H]/dt)/(d[P_D]/dt)$, or, more simply, k_H/k_D.]

EXPERIMENTAL PROCEDURES

Materials. Phenylalanine dehydrogenase (PheDH) was prepared according to the procedures of Brunhuber et al. (*11*). The enzyme preparation was dialyzed against three changes of 0.1 M TEA and 0.1 M NaCl at pH 8.0 under 5 °C, centrifuged at 2000 rpm for 20 min, and pushed through a 0.45 μm filter. The concentration of the enzyme was determined spectrophotometrically at 280 nm (ε = 22.12 cm^{-1} mM^{-1}). TEA, NaCl, phenylpyruvate (PhePyr), NAD, NADH, and h-L-phenylalanine (h-L-Phe) were obtained from Sigma, and L-phenylalanine (2-D 98%) (d-L-Phe) was from Cambridge Isotope Laboratories.

Transient-State Kinetics. The transient-state absorbance versus wavelength and time array was obtained using an Applied Photophysics SX-18MV stopped-flow apparatus by assembling a series of side-by-side single-wavelength time traces, in which a solution containing enzyme and h- or d-L-Phe in one syringe is mixed with a solution containing enzyme and NAD in the other. The spectra were collected at 1 nm and 0.05 ms intervals. An individual experiment such as that portrayed in Figure 3a takes approximately 20 min to produce an array comprising 121600 individual points, each of which is an average of three successive photomultiplier readings. This reaction was carried out at pH 8.0,

†This work was supported by the University of Kansas Medical Center, Kansas City Veterans Affairs Medical Center, and NIH Grant R01GM081374.

*To whom correspondence should be addressed. Telephone: (913) 945-6782. Fax: (913) 588-9896. E-mail: hfisher@kumc.edu.

[1]Abbreviations: A, L-amino acid; C, α-carbinolamine; E, enzyme; GDH, glutamate dehydrogenase; I, α-imino acid; iss, isotope sensitive step; K, α-keto acid; KIE, kinetic isotope effect; N, ammonia; O, NAD(P); PheDH, phenylalanine dehydrogenase; P, product; R, NAD(P)H.

Published on Web 11/19/2009

10 °C, in a 0.1 M TEA and 0.1 M NaCl buffer. The final reactant concentrations after mixing were 45 μM PheDH, 1.0 mM NAD, and 1.0 mM h- or d-L-Phe.

Deconvolution of Reaction Spectra Observed at Specific Individual Times into Spectral Components. Full spectra obtained at intervals of 0.05 ms were each deconvoluted into sums of the contributions of individual spectral components according to their agreement with a multiwavelength form of Beer's law. This process has been described in detail in ref *6*. Individual model spectra were obtained in the following way: All model experiments were run in 0.1 M TEA and 0.1 M NaCl at pH 8.0 and 20 °C. The models of component spectra shown in Figure 3b were obtained by difference spectroscopy using a Cary 300 spectrophotometer. The NADH model was 50 μM with an extinction coefficient of 6.22 cm^{-1} mM^{-1} and a λ_{max} = 339 nm. Binding constants were determined for the ERPhe model at 8 μM with an extinction coefficient 5.85 cm^{-1} $mM^{-1}$and a λ_{max} = 343 nm within a range of NADH concentrations from 0 to 90 μM in the presence of 12 μM PheDH and 1 mM L-Phe. The ERPhePyr model was determined at 8 μM with an extinction coefficient 5.72 cm^{-1} mM^{-1} and a λ_{max} = 337 nm within a range of NADH concentrations from 0 to 30 μM in the presence of 10 μM PheDH and 1 mM L-PhePyr. The results of this analysis at specific points in time were then combined along the time axis to provide spectral time courses. It is to be understood that any given spectral component may contain contributions from several species having indistinguishable spectra. The relative amounts of the contributions of such species will, however, vary with time and may thus be distinguished kinetically.

Kinetic Resolution of Spectral Component Time Courses. The experimental data now represented by spectral component time courses are then fitted to the set of ordinary differential equations corresponding to the minimal reaction mechanism which accounts for the thus far known facts. To this end, the scan data were deconvoluted by solving the data matrixes with known vectors provided by the component spectra models using the Matlab program (Mathworks, Natick, MA). The criterion for the fit solution is based on the lowest trended residuals to a multiwavelength Beer's law function. The Jacobian matrix is generated from the analytic forms of the partial derivatives with respect to time. Treating this matrix as banded, we apply, using the Scientist program (MicroMath, St. Louis, MO), variable-coefficient simplex minimization and simplex fitting to solve for the rate constants. The "first rule" is applied to the first-order derivatives of the synthetic results. The "second rule" is then applied to the first derivatives of the tKIEs in order to approximate the isotope sensitive step by comparing the step predictions to the integral values (or the integral results from the multiplied fractional values). A new set of equations are generated based on the modified kinetic scheme which is then again fit with the deconvoluted spectral components. This entire process is repeated until the second rule is satisfied with integral results.

RESULTS

The First Rule of Transient-State tKIEs. This rule states that for any *post*-isotope-substituted linear reaction sequence:

$$\lim_{t \to 0} \mathrm{tKIE_X} = \mathrm{KIE_{int}} \tag{1}$$

For any *pre*-isotope-substituted step in such a reaction:

$$\lim_{t \to 0} \mathrm{tKIE_X} = 1 \tag{2}$$

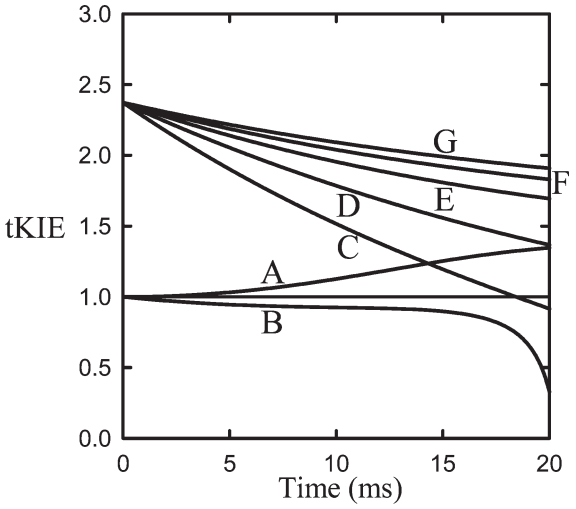

FIGURE 1: Application of the first rule to an assumed reaction mechanism:

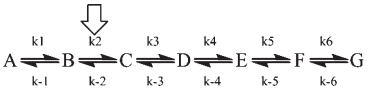

where the vertical arrow designates the isotope sensitive step (iss). The first rule time courses of tKIEs of the reaction components were calculated according to eqs 11 and 22 by numerical integration. This example assumes an intrinsic KIE = 2.3, and the iss in this case is step 2.

Simulations based on numerical integration of kinetic models with widely varying combinations of rate constants and over a wide range of assumed intrinsic KIE values have failed to find any exception to the validity of this rule (*5*). An example of one such simulation is shown in Figure 1.

Formal analytical proof of eqs 1 and 2 has been obtained without the requirement of any assumptions other than that of the mass law itself (*4*). Their correctness has been experimentally supported for several pyridine nucleotide linked dehydrogenases (*6*, *7*).

The Second Rule of Transient-State tKIEs[2]. This rule states that for such reactions:

$$n_S = I\left[\frac{\lim_{t \to 0} \mathrm{d(tKIE_1)/d}t}{\lim_{t \to 0} \mathrm{d(tKIE_2)/d}t}\right] \tag{3}$$

where n_S is the number of the step in the reaction sequence whose product formation follows k_n and I is an integer equal to the number of steps preceding and including the isotope sensitive step (iss). In the course of calculating tKIEs from our experimental data we noticed that while the first rule (that the tKIEs for all components converged to a common value at $t = 0$) appeared to hold true, the time courses of those individual tKIEs exhibited a peculiar pattern. The tKIEs for the first formed complex in the reaction sequence fell quite rapidly in time, but those of the following complexes fell at successively slower rates. A computer simulation of the reaction shown in the legend to Figure 1 assuming a KIE of 2.3 occurring in the first step proved that the ratios of the limits of d(tKIE) as $t \rightarrow 0$ did indeed form a series of 2, 3, and 4 for n_S precisely, as shown in Figure 2.

If the isotope effect happens to occur in the second step rather than in the first as we have assumed with $I = 1$, we now obtain the

[2]Equation 3 (the definition of the second rule) has been modified from its original form in ref *4* by incorporating the variable integer *I* into the expression.

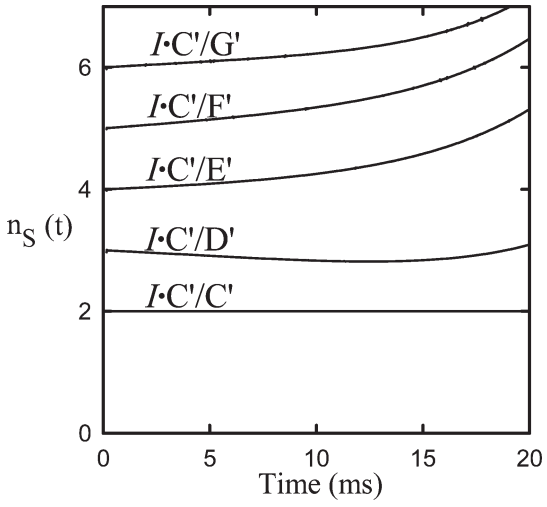

FIGURE 2: The second rule time courses of the first derivatives of the tKIEs multiplied by I as in eq 3. I is set to a value of 2 here as required by the location of the iss in this example.

nonintegral values of n_S of 1, 1.5, 2, and 2.5 instead of 1, 2, 3, and 4, the set of simple integers required by the second rule. However, setting $I = 2$, n_S now provides the appropriate series of integers corresponding to each of the steps in the mechanism. In such a case, multiplication of each n_S by an integer (2, 3, or 4) produces an exact integral value which corresponds to the step number for that species in the postulated reaction mechanism. If this procedure fails, then additional steps must be added at the appropriate places in the mechanism until eq 3 is satisfied. Thus, the second rule has the ability to use kinetic data from those complexes that can be observed to test their kinetic competence and to predict the occurrence and mechanistic location of complexes that have not yet been observed as well!

As in the case of the first rule, both digitally integrated simulations and a rigorously derived formal proof of the validity of this counterintuitive second rule have been provided (*4*). Our purpose here is to test its force and predictive precision experimentally and to demonstrate the ability of the combined application of the first and second rules to provide a novel and potentially powerful approach to the mechanistic resolution of complex chemical reactions. The evaluation of the $t \rightarrow 0$ limits of these complex equations leads to much simpler and more tractable forms.[3] We demonstrate here its ability to apply both of these properties to actual experimental data.

The Development and Application of a Rigorous Approach to the Resolution of Multiwavelength Transient-State Time-Course Arrays into Kinetically Competent Sequences of Physically Identifiable Intermediate Complexes. We have developed an approach which we believe to be quite rigorous and free of the limitations of current practices in transient-state methods, as discussed in ref *2*. This method, "the resolved component time-course approach" employs the following basic experiment: Using a stopped-flow apparatus in which a solution containing enzyme and substrate in one syringe is mixed with a solution containing the coreactant and an equal concentration of enzyme in the other, we obtain a transient-state absorbance vs wavelength and time array. We also determine the corresponding array from the α-deuterio-substituted reaction.

The analysis of such an array (described in detail in ref *7*) involves three successive processes: (1) the qualitative and quantitative deconvolution of each observed spectrum (time slices of the array) into the individual components, each having a known shape and extinction coefficient whose individual contributions account quantitatively for the spectrum observed experimentally at any given point in time; (2) the assignment of each of these components to a known or postulated reactive enzyme complex; (3) the determination of the kinetic competence of each of these species in occupying their postulated positions along the reaction time course. To apply a further constraint to the solution, we solve the data from an α-deuterio substrate reaction and from an α-protio one simultaneously, permitting only the two constants of the hydride transfer step to vary. Solving the now highly constrained set of differential equations for an assumed mechanism by means of computer-run matrix manipulation, we have obtained mechanisms involving five kinetically competent complexes in the chemical interconversion portion of both the bovine liver and *Clostridium symbiosum* glutamate dehydrogenase reactions (*6*, *7*).

Application of the First and Second Rules To Resolve the Mechanism of a Pyridine Nucleotide Linked α-Amino Acid Dehydrogenase Reaction. The stoichiometry of this class of enzyme reactions is

$$\underset{\mathbf{A}}{\text{L-amino acid}} + H_2O + \underset{\mathbf{O}}{\text{NAD(P)}} \rightleftharpoons \underset{\mathbf{K}}{\alpha\text{-keto acid}} + \underset{\mathbf{N}}{NH_3} + \underset{\mathbf{R}}{\text{NAD(P)H}} + H^+ \quad (4)$$

The bold letters shown below each species will be used throughout this report. **A** is L-amino acid, **K** is α-keto

[3] Based on the mass law, eq 8 represents the exact solution of the set of differential equations that describe the kinetic behavior of any reaction of n steps that can be written:

$$v = \frac{d[P]}{dt} = \sum_{i=1}^{n} a_1 e^{-\lambda t} \quad (8)$$

Each step of any such reaction contributes one exponential term ($e^{-\lambda t}$) to the equation. The numerical values of the λ terms are those of the exponentials observed in the transient-state experiment. These values, however, do not in the general case represent a rate constant of a specific step (a common and invalid assumption seen frequently in the current literature of the field). The λs are in fact eigenvalues of a entire reaction, reflecting the harmonics of a multicomponent oscillator system and do not correspond individually to any identifiable mechanistic feature. By evaluating the kinetic equations at the $\lim_{t\rightarrow 0}$, all of the λ functions become unity, effectively removing the exponential terms completely and reducing the complexity of the remaining preexponential terms by a considerable amount, since the λs also occur in various combinations there. Mathematicians have struggled for two centuries over attempts to deal with equations of the form of eq 8. The state of current approaches to the A ⇌ B ⇌ C problem has been summarized by Windig (*12*). It has been proven that the two-step reversible reaction is the largest reaction for which a closed integral solution to eq 8 exists. Even in this simple case the integral equation involves over 700 terms, each of which involves multiple combinations of all four rate constants. The point has been discussed in some detail in analytic form by Moore and Pearson (*13*) and more briefly in ref *2*. It has also been shown that many quite different mechanisms are described by the same mathematical expression. The only exception to this degree of complexity occurs where a particular intermediate is harmonically uncoupled from the other entities in the reaction sequence. The most common case of such an event is the release of a product into a pool of zero concentration. A 10-fold disparity of forward and reverse rate constants would also substantially eliminate coupling. Such cases are rarely observed. Restating the problem in experimentally approachable terms, the solution of an n-step reaction involves the simultaneous solution of n differential equations, and that operation requires the availability of n independent phenomenological sets of experimental results. Our approach as described here involves a series of optical and analytical operations, each of which provides a mathematical constraint to eq 8 and applied sequentially reduces the otherwise intractable mathematical complexity by geometrically increasing degrees. Here, we apply spectroscopic resolution, component and spectroscopic models, and isotopic substitutions to produce a second step of component time courses and SVD analysis. These constraints, while helpful, are insufficient to establish a realistic mechanism in this case. Application of the first and second rules to transient-state isotope effects does accomplish this task.

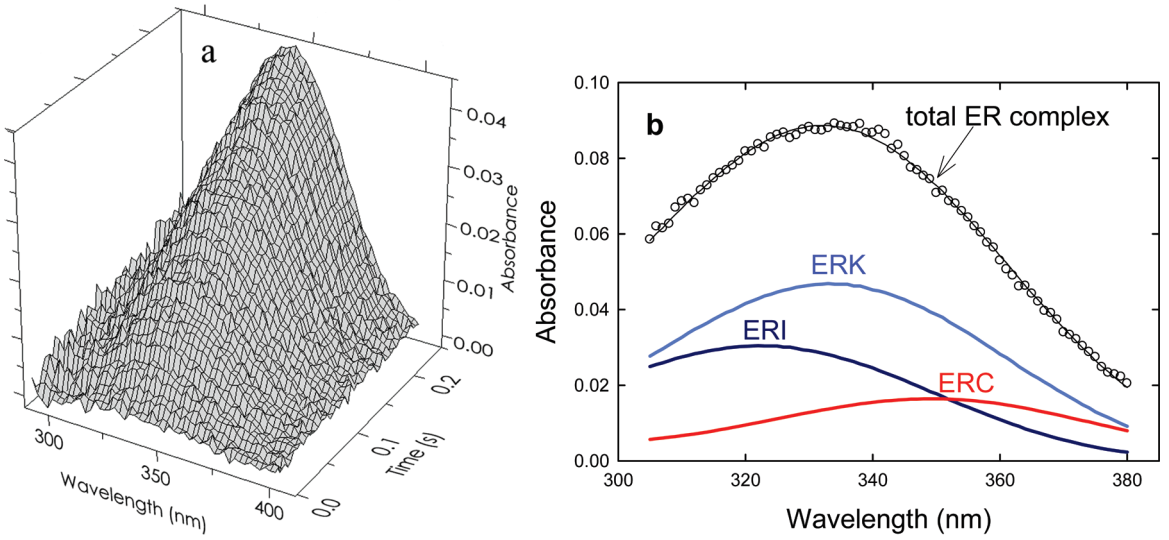

FIGURE 3: (a) Time and wavelength dependence of the optical absorbance of the phenylalanine dehydrogenase catalyzed reaction. The array, composed of 121600 experimental points, has been parsed here for clarity. (b) The resolution of a typical spectrum in (a) at a single point in time (80 ms) is indicated by the open circles. The shapes of the model spectra of the components were determined as described in the Experimental Procedures section. Their amplitudes were adjusted so as to obtain Beer's law compliance as shown by the solid line through the open circles.

acid, **N** is ammonia, **O** is NADP (oxidized coenzyme), and **R** is NAD(P)H (reduced coenzyme). The basic chemical mechanism has been shown to be (*6*−*11*)

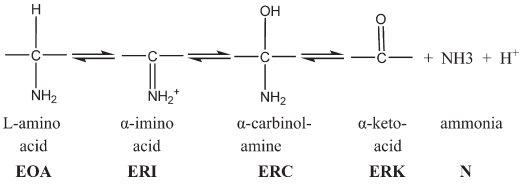

(5)

[The boldface abbreviations in these two equations will be used throughout the following discussion.] Other members of the class have similar active site structures, and their reactions involve the same sequences of complexes. The kinetics of the various enzymes, however, vary considerably.

While the cs-GDH reaction time course was solved with relative ease due to the abundance of five spectroscopically distinguishable and kinetically separable components without the aid of a deuterio substitution, the attempt to solve the mechanism for the closely related phenylalanine reaction in this manner provided some difficulties. The three-dimensional array of absorbance vs wavelength and time for the PheDH reaction is shown in Figure 3a. A corresponding array for the same reaction using α-deuterio- (D-) substituted L-α-phenylalanine was also obtained (data not shown).

Having applied the three steps of our standard resolution procedure we have described earlier to this reaction, our best fit to the first 200 ms of the data revealed only two spectral components, one, a slightly red-shifted peak, and the second, a slightly blue-shifted peak, in contrast to the more separable spectra of bl- and cs-GDH observed in refs *6* and *10*. A representative resolution of the spectrum obtained at a single point in time is shown in Figure 3b. A plot of the time courses of the two components for both the H- and D-substituted reactions in their early time periods is shown in Figure 4.

[4]It may be presumed that each of the three simple exponentials used to provide the individual component time courses in Figure 4 either are or are closely related to their eigenvalues.

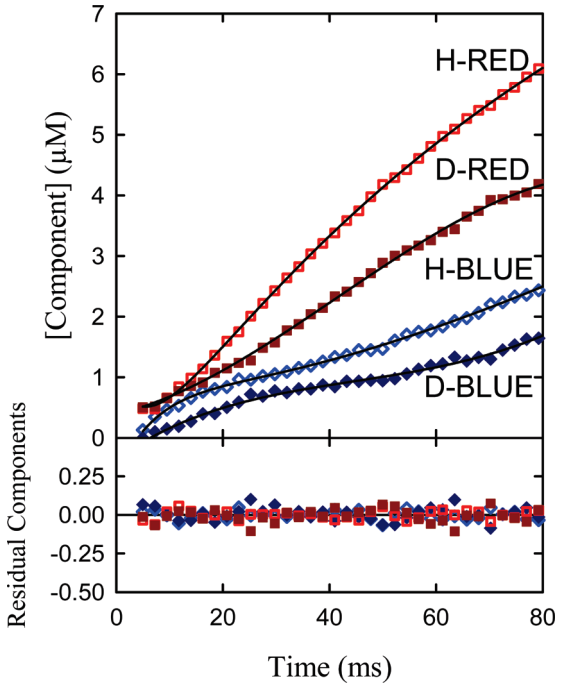

FIGURE 4: Time courses of the red- and blue-shifted components of both the protio- and α-deuterio-substituted L-phenylalanine.

It should be noted that these simplistic two-exponential fits are applied independently to each curve as smoothing functions; no specific kinetic relationships have been imposed or implied at this point.[4]

Having consolidated the experimental data into a manageable form, we proceed to apply the first and second rules to obtain a mechanism composed of a set of kinetically competent intermediate complexes. In this process all four of the H and D and the blue- and red-shifted complexes are fitted simultaneously to the set of differential equations representing a given multistep reaction mechanism. Each enzyme complex is represented as having a red- or blue-shifted NADH spectrum according to models either obtained by direct measurement of relevant PheDH complexes or inferred from previous results from closely

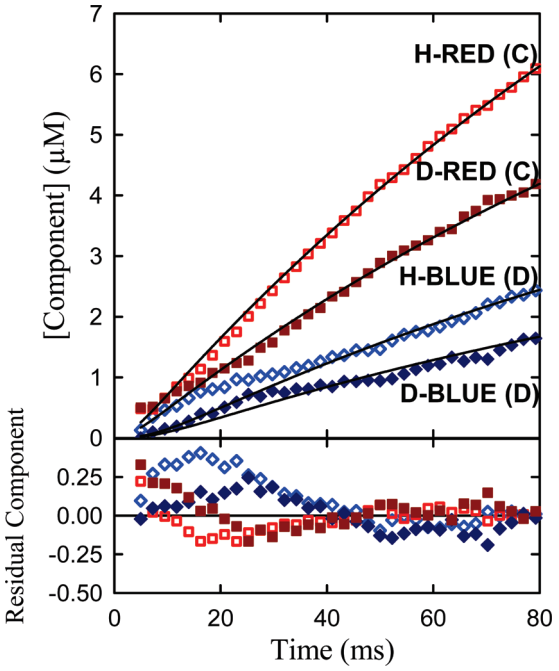

FIGURE 5: A simultaneous fit of all four traces shown in Figure 3 to the three-step mechanism shown in eq 6, where C and D follow the red and blue components.

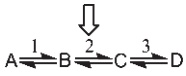

(6)

related enzymes and located along the reaction pathway by correlating their observed order of appearance with the chemical events required by eq . One such simultaneous fit is shown in Figure 5.

The substantial degree of trended residuals to the fit in Figure 5 indicates that a three-step mechanism is inadequate to account for the experimental data. Attempts to fit all of the components from both the protium and deuterium data sets successively with four and five step linear kinetic reaction equations produced increasingly better fits but failed to meet the more stringent requirements of the second rule.[5] Application to a six-step reaction scheme, however, was successful. After obtaining the component tKIE time courses by dividing data of the α-protium reaction by that of the corresponding α-deuterio-substituted set and applying the first rule to obtain accurate zero-time intercepts, we obtain the curve shown in Figure 6a.

The first derivatives of the component tKIEs are shown in Figure 6b. Application of the second rule (eq 3) to these zero-time intercepts with "*I*" assumed to have the value of 1 initially provided the n_S time courses shown by the dotted lines in Figure 6c. Since the set of zero-time n_S values contained nonintegers, we now follow the requirements of the second rule and set the value *I* to successive integers. Setting $I = 3$ produces the solid line curve of Figure 6c whose intercepts for the posthydride complexes are precisely 3, 4, 5, and 6. Thus, the application of the second rule has deduced the existence of two new reaction steps, one involving a pre-hydride complex and the second reflecting a post-hydride entity.

On this basis we now propose an expanded minimal mechanism for the early steps of the PheDH-catalyzed reaction shown in eq 7.

[5]The characteristic of having "the ability to fail" when presented with data unsuited to its intrinsic form is an important feature of an analytic equation and demonstrates the absence of overall circularity in its argument.

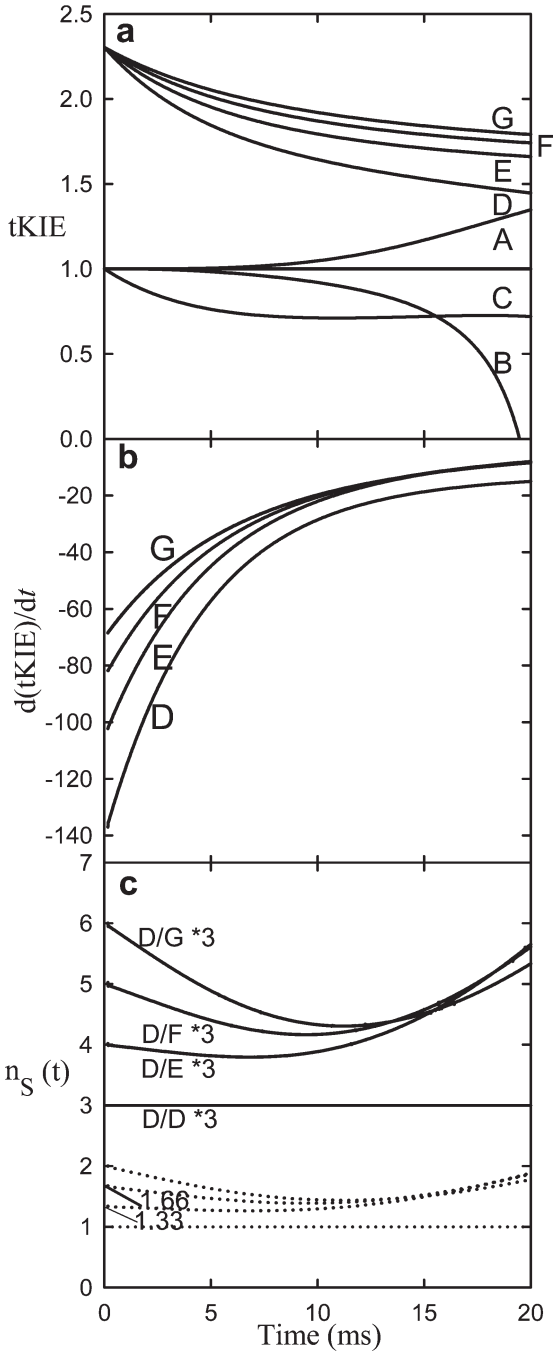

FIGURE 6: Application of the first and second rules to the phenylalanine dehydrogenase reaction. (a) Application of the first rule time courses of tKIEs of the reaction components assuming the six-step mechanism of eq 8. (b) First derivatives of the component tKIE time courses of panel a. (c) Application of the second rule. n_S is calculated according to eq 3 with $I = 1$ (dotted lines) yielding nonintegral n_S intercepts and with $I = 3$ (solid lines) yielding integral n_S intercepts.

The fit of this equation to the experimental data and the residuals of that fit (lower panel) are shown in Figure 7.[6]

[6]The individual rate constants that define the fit in Figure 7 listed in the figure legend are individual microconstants and are not assumed to have any real mechanistic significance; the fit implies only that there does exist at least one set of numbers that satisfy the relationship of the equation to the data. It is unlikely that this particular set is unique. Indeed, "kinetic flip-flopping" between pairs of rate constants of well-separated steps in a reaction scheme is a quite commonly observed kinetic event.

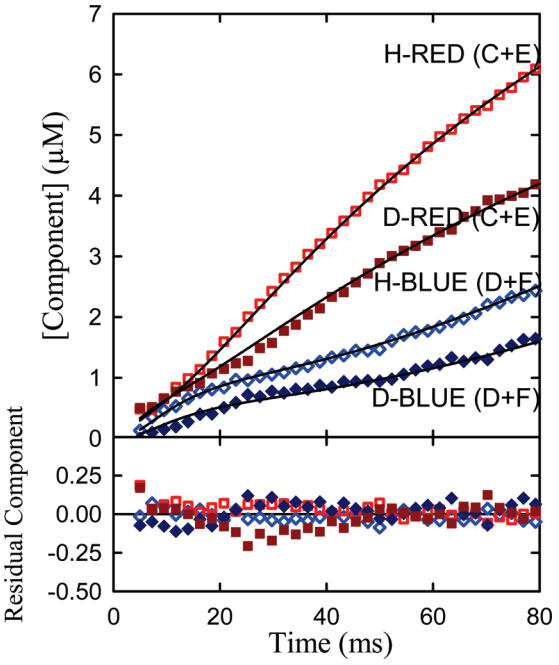

FIGURE 7: Simultaneous fit of all four components to an expanded mechanism (eq 7), where "H" and "D" refer to spectroscopically resolved components of the α-protio and deuterio reactions, respectively (*5*). Rate constants for the fit of eq to the component curves of Figure 7: $k_1 = 66$, $k_{-1} = 164$, $k_2 = 27$, $k_{-2} = 388$, $k_3 = 291$, $k_{3iso} = 127$, $k_{-3} = 31$, $k_4 = 130$, $k_{-4} = 9$, $k_5 = 7$, $k_{-5} = 3$, $k_6 = 2$, and $k_{-6} = 26$.[6]

On the basis of the order of appearance observed experimentally, and the correspondence of their spectra to those of model complexes, on the known chemistry of the reaction and on the location of the iss, we now assign the individual complexes to the lettered sequence in eq 7.

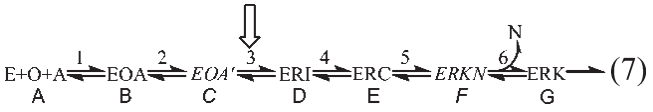

The resolved components' spectra and time courses corresponding to eq 7 are portrayed in Figure 8. It can be seen that Figure 8 represents the resolution of the absorbance vs time and wavelength array shown in Figure 3a. The EOA′ pre-hydride transfer entity shown in Figure 8 would appear to be a charge transfer complex. Its relatively slow development suggests that its formation involves a change in the conformation of the preceding EOA′ complex. In turn, that complex, which is not observed directly but whose presence is revealed by application of the second rule itself, appears to form by yet another change in the conformation of an initial encounter complex not indicated in eq 8.

Thus, we have demonstrated the applicability of the second rule of the transient-state kinetic isotope effects to the experimental data of an enzymatic reaction. The potential power of this rule is made evident by its success in resolving a case in which only two spectroscopic signals were initially available, in contrast to the more easily resolved reactions, each of which provided five independent such signals.

PERSPECTIVE

Finally, we note some inherent limitations and some potentially useful extensions to both the scope of the applicability and

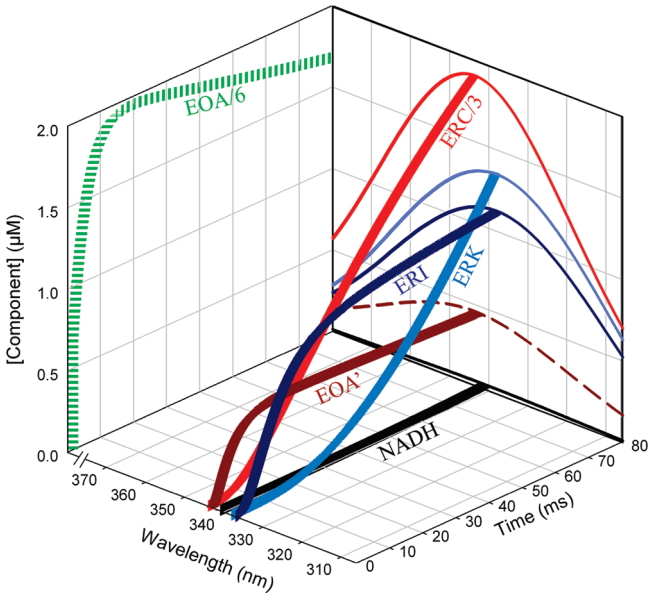

FIGURE 8: Time courses and spectra of kinetically competent complexes in the early portion of the Phe-catalyzed reaction. The dashed band indicates a pre-hydride transfer complex; the solid bands indicate post-hydride transfer entities. Resolved spectra of individual complexes observed at 80 ms are portrayed on the rear plane.

the mechanistic resolving power of the second rule. Buried in the mathematical structure is the restriction that the second rule limits itself to defining only the shortest viable mechanistic pathway from the reactants to products, ignoring all longer kinetic component pathways even in cases where such a pathway provides a faster overall reaction. While the application of this rule does reduce the fitting deviations shown by the time-course residual plots, certain small local deviations remain despite experimental repetition and recursive data fitting procedures. These apparently nonrandom deviations could arise from experimental error such as inexactness of our component spectroscopic models, or they could equally well arise from alternative mechanistic loops ignored by the second rule but nevertheless contributing to the observed reaction. On the positive side, the approach may be extended to other stable and even radioactive nuclei with only minor mathematical elaboration. Since our intent here is to demonstrate the applicability of the second rule itself, we have purposely limited the results presented to a single optical signal (multiwavelength absorbance) and to the limited time range, ignoring the multiple product release steps evident at substantially later reaction times. This demonstration completes the proof of applicability for each of the three rules of transient-state kinetic isotope effects which we proposed (*3*). We suggest that these three rules may serve as a starting point for the future development of a general rigorously derived and experimentally applicable theory of transient-state multistep kinetics, as up to this time none has been available.

ACKNOWLEDGMENT

We thank Janine Vanhooke for advice on the production and purification of phenylalanine dehydrogenase.

REFERENCES

1. Cook, P. F., and Cleland, W. W. (2007) Enzyme Kinetics and Mechanism , Garland Science Publishing, London and New York.
2. Fisher, H. F. (2005) Transient-state kinetic approach to mechanisms of enzymatic catalysis. *Acc. Chem. Res. 38*, 157–166.

3. Cook, P. F. (1991) Enzyme Mechanism from Isotope Effects, CRC Press, Boca Raton, FL.
4. Fisher, H. F., Palfey, B. A., Maniscalco, S. J., and Indyk, L. (2006) Relationship between the time-dependence of a transient-state kinetic isotope effect and the location of complexes in a reaction sequence. *J. Phys. Chem. A 110*, 4465–4472.
5. Maniscalco, S. J., Tally, J. F., and Fisher, H. F. (2004) The interpretation of multiple-step transient-state kinetic isotope effects. *Arch. Biochem. Biophys. 425*, 165–172.
6. Maniscalco, S. J., Saha, S. K., and Fisher, H. F. (1998) Identification and characterization of kinetically competent carbinolamine and α-iminoglutarate complexes in the glutamate dehydrogenase-catalyzed oxidation of L-glutamate using a multiwavelength transient state approach. *Biochemistry 37*, 14585–14590.
7. Saha, S. K., and Fisher, H. F. (1999) The location of active site opening and closing events in the prehydride transfer phase of the oxidative deamination reaction catalyzed by bovine liver glutamate dehydrogenase using a novel pH jump approach. *Biochim. Biophys. Acta 1431*, 261–265.
8. Rife, J. E., and Cleland, W. W. (1980) Kinetic mechanism of glutamate dehydrogenase. *Biochemistry 19*, 2321–2328.
9. Stillman, T. J., Baker, P. J., Britton, K. L., and Rice, D. W. (1993) Conformational flexibility in glutamate dehydrogenase. Role of water in substrate recognition and catalysis. *J. Mol. Biol. 234*, 1131–1139.
10. Tally, J. F., Maniscalco, S. J., Saha, S. K., and Fisher, H. F. (2002) Detection of multiple active site domain motions in transient-state component time courses of the *Clostridium symbiosum* L-glutamate dehydrogenase-catalyzed oxidative deamination reaction. *Biochemistry 41*, 11284–11293.
11. Brunhuber, N. M., Thoden, J. B., Blanchard, J. S., and Vanhooke, J. L. (2000) *Rhodococcus* L-phenylalanine dehydrogenase: kinetics, mechanism, and structural basis for catalytic specificity. *Biochemistry 39*, 9174–9187.
12. Windig, W., and Antalek, B. (1999) Resolving nuclear magnetic resonance data of mixtures by 3-way analysis. examples of chemical solutions and the human brain. *Chemom. Intell. Laboratory Syst. 46*, 207.
13. Moore, J. W., and Pearson, R. G. (1981) Kinetics and Mechanism, 3rd ed., Wiley, New York.